Progress in x-ray critical-angle transmission grating technology development

Ralf K. Heilmann[a], Alexander R. Bruccoleri[b], Jungki Song[a], and Mark L. Schattenburg[a]

[a]Space Nanotechnology Laboratory, MIT Kavli Institute for Astrophysics and Space Research, Massachusetts Institute of Technology, Cambridge, MA 02139, USA
[b]Izentis, LLC, Cambridge, Massachusetts 02139, USA

ABSTRACT

High resolution absorption and emission line spectroscopy in the soft x-ray band are promising techniques to measure hot baryon distributions in extended galaxy halos, galaxy clusters, and the connecting filaments of the cosmic web. It can characterize outflows from supermassive black holes and help understand their impact on the structure and evolution of the interstellar medium and beyond. Stellar magnetic activity, accretion, coronal emission and flares are additional targets for soft x-ray spectroscopy. Higher resolving power and larger effective area than those provided by current missions are required in order to make progress. Recent breakthroughs in x-ray diffraction grating and mirror technologies promise order-of-magnitude improved performance if new missions were built today, and even greater improvements beyond the next decade. Here we describe recent progress in critical-angle transmission (CAT) grating technology. CAT gratings combine the advantages of traditional transmission gratings (relaxed alignment tolerances, low mass, transparency at higher energies) and blazed reflection gratings (high diffraction efficiency, high resolving power R due to blazing into high orders). CAT gratings have demonstrated resolving power greater than 10,000 and absolute diffraction efficiency above 30% in the soft x-ray band. They are an enabling technology for the Arcus grating spectrometer Explorer ($R >$ 2500, effective area $>$ 250 cm^2) and a candidate for the Lynx x-ray grating spectrometer ($R >$ 5000, effective area $>$ 4,000 cm^2).

Keywords: Arcus, Lynx, critical-angle transmission grating, x-ray spectroscopy, blazed transmission grating, soft x-ray, grating spectrometer, high resolving power

1. INTRODUCTION

Astronomers believe the majority of baryonic matter in the universe to be "hidden" in hot plasmas too faint to detect with current instruments. The high temperatures of these plasmas lead to highly ionized states of many of the most abundant "metals" (O, C, Ne, Fe, N, Si, Mg, S) with spectral lines in the soft x-ray band between $\sim$ 0.2 - 2.0 keV. The science cases alluded to in the abstract of this paper have been described in detail by Smith[1] and Bautz[2] and references therein and call for spectral resolving power $R = \lambda/\Delta\lambda$ in the range of 2000 - 5000 and effective area A_{eff} of hundreds to thousands of cm^2, depending on the target luminosity and available exposure times.

Resolving power $R > 800$ below 2.0 keV currently can only be achieved using dispersive grating spectrographs for missions proposed to launch within the next decade and a half. However, existing instruments (the Chandra High Energy Transmission Grating Spectrometer (HETG)[3] and the XMM-Newton Reflection Grating Spectrometer (RGS),[4] both launched 20 years ago) represent technology from a generation ago and fall woefully short in R ($\sim 100 - 1500$), effective area ($\sim 10 - 100$ cm^2) and relevant figures of merit (e.g. $\sqrt{(RA_{eff})}$) to address current science questions. Thankfully, breakthroughs in x-ray grating and mirror technologies over the last decade allow us to build missions today that are an order of magnitude more powerful than the observatory-class missions of yore, but within a much smaller NASA Explorer budget.

Further author information: (Send correspondence to R.K.H.)
E-mail: ralf at space.mit.edu, , URL: http://snl.mit.edu/

Optics for EUV, X-Ray, and Gamma-Ray Astronomy IX, edited by Stephen L. O'Dell, Giovanni Pareschi, Proc. of SPIE Vol. 11119, 1111913 · © 2019 SPIE · CCC code: 0277-786X/19/$21 · doi: 10.1117/12.2529354

The Arcus[1] soft x-ray grating Explorer mission concept features a modular design with four parallel optical channels, each consisting of a co-aligned array of 12 m-focal length silicon pore optic (SPO) mirror modules,[5] developed in Europe for the Athena[6] mission. Just aft of each mirror array follows an array of critical-angle transmission (CAT) gratings arranged on the surface of a tilted Rowland torus.[7–9] Two CCD readout arrays together collect the four spectra generated by the four channels. CAT gratings, under development for over ten years, have achieved high technical maturity, and current gratings provide flight-ready performance for Arcus. They combine the advantages of traditional transmission gratings (relaxed alignment tolerances, low mass, transparency at higher energies) and blazed reflection gratings (high diffraction efficiency, high resolving power R due to blazing into high orders). This unique combination of properties allows for the cost-effective implementation of CAT grating arrays in tandem with industrially produced SPOs (point spread function (PSF) $<$ 2 arcsec full width half max (FWHM) in the dispersion direction) to enable a mission with $R > 2500$ and effective area $A_{eff} > 250$ cm^2 over most of the 0.25 - 1.5 keV band.

Lynx[10] is a large x-ray telescope mission concept proposed for the 2020 Astrophysics Decadal Review, with an envisioned launch date in the 2030's. With a mirror collecting area ~ 2 m^2 and a PSF ~ 0.5 arcsec it also features a grating spectrometer as one of its candidate instruments. Being able to take advantage of such a large collecting area and narrow PSF, it is very feasible to design a CAT grating spectrometer with the required 4000 cm^2 A_{eff} and $R > 5000$, with a goal of $R = 7500$. Realistic improvements in grating performance will lead to a grating array consisting of $\sim 1000 - 2000$ CAT grating facets with fairly relaxed alignment tolerances and temperature stability and gradient requirements.[11] This instrument has been selected for the Design Reference Mission described in the Lynx X-ray Observatory Report.[12] A detailed Technology Development Roadmap that can take CAT grating technology from today's state-of-the-art (Technology Readiness Level (TRL) 4) to TRL 6 for Lynx by 2024 has been developed.[13]

In the following we will briefly review the state-of-the-art (SOTA) of CAT grating technology. We will then discuss the necessary performance improvements to meet the requirements for Lynx and our efforts to prepare for mass-production of CAT gratings. Recent progress along those lines will be described before we summarize.

2. CAT GRATING TECHNOLOGY STATE-OF-THE-ART

CAT gratings were invented in 2005 and have been under funded development since 2007. Support under NASA's APRA and SAT programs has been essential to bring the technology to TRL 4 in 2016 and for it to become an enabling technology for the Arcus mission.

2.1 CAT grating design

CAT gratings consist of ultra-high aspect-ratio, freestanding grating bars with nm-smooth sidewalls. The gratings are aligned such that x rays are incident onto the sidewalls at a graze angle θ below the critical angle for total external reflection (see Fig. 1). This leads to efficient blazing into diffraction orders near the direction of specular reflection from the sidewalls. For most efficient blazing each photon that enters the space between two grating bars should encounter the same sidewall once. Due to the small critical angles for soft x rays (typically on the order of 1-2 degrees) this demands high aspect ratio grating bars. Furthermore, the bars should be as thin as possible to minimize absorption. Finally, the grating period cannot be too large compared to the x-ray wavelength to obtain useful diffraction orders. For Arcus this led us to a design with grating period $p = 200$ nm, grating bar depth $d = 4$ micrometers, and bar thickness $b \approx 60$ nm. Such a grating is most efficient when $\tan\theta \approx (p - b)/d$, or $\theta \approx 2$ deg.

2.2 Grating fabrication

We have fabricated numerous CAT gratings with these parameters in sizes up to 32×32 mm^2.[14,15] We start with a silicon-on-insulator (SOI) wafer with a (110) device layer (front side) of thickness d, a thermal oxide layer on both sides, and an additional plasma-enhanced chemical vapor deposition (PECVD) oxide layer on the back (see Fig. 2). The grating pattern is defined lithographically, with grating lines parallel to one set of vertical {111} planes. A cross-support mesh (period = 5 μm) is defined in similar fashion. The combined pattern is transferred into the thermal oxide, which serves as a mask for the subsequent deep reactive-ion etch (DRIE). The buried oxide (BOX) layer serves as an etch stop. This is followed by a short anisotropic wet etch in KOH

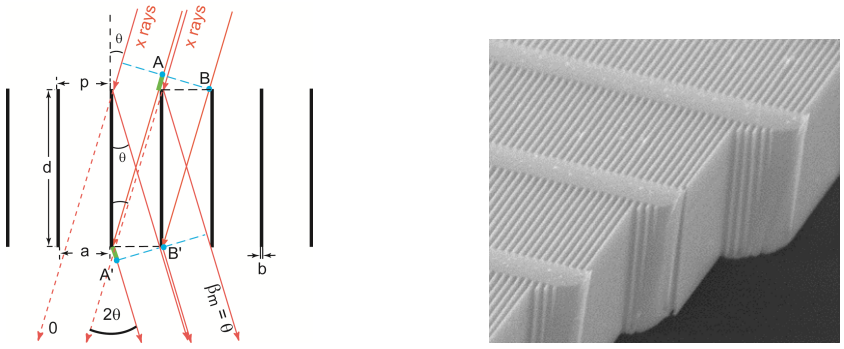

Figure 1. Left: Schematic cross-section through a CAT grating of period p. The m^{th} diffraction order occurs at an angle β_m where the path length difference between AA' and BB' is $m\lambda$. Shown is the case where β_m coincides with the direction of specular reflection from the grating bar sidewalls ($|\beta_m| = |\theta|$), i.e., blazing in the m^{th} order. Right: Scanning electron micrograph of a cleaved CAT grating membrane showing top, cross-section and sidewall views of the 200 nm-period silicon grating bars and their monolithically integrated 5 μm-period cross supports (x rays enter from the top and leave out the bottom).

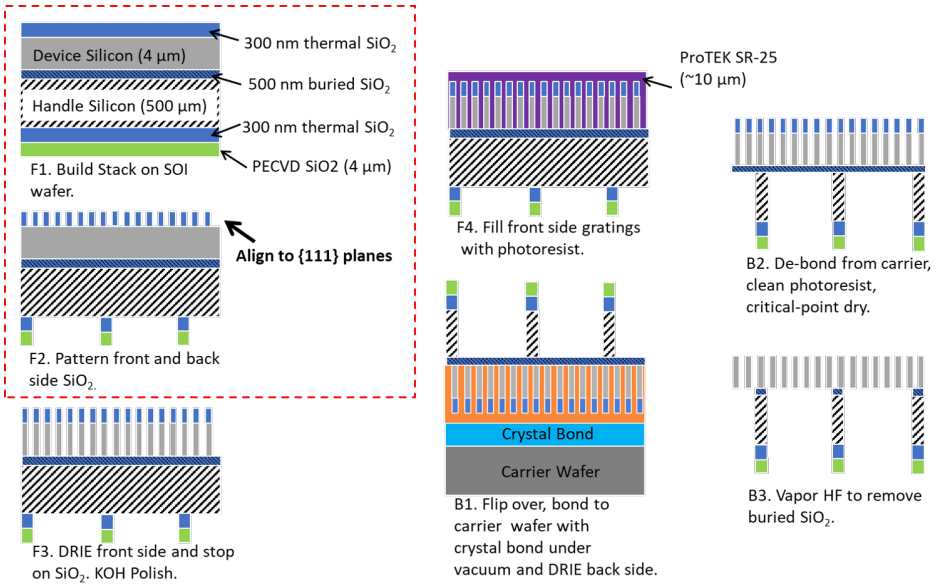

Figure 2. Highly simplified schematic overview of CAT grating fabrication steps. See text for more details.

solution, which greatly reduces the scalloping from the DRIE and leaves smooth {111} grating bar sidewalls. The front side is protected and bonded to a carrier wafer. The back side PECVD oxide is patterned into a coarse (pitch $\sim$ 1 mm) hexagon mesh, surrounded by a narrow frame area. This pattern is etched through the $\approx$ 500 μm-thick handle layer using DRIE, again using the BOX layer as an etch stop. Then the wafer is detached from the carrier, cleaned, and critical-point dried. The BOX layer is removed from the open areas using HF vapor etching, resulting in a freestanding grating with integrated Level 1 (L1) cross-supports and a strong Level 2 (L2) hexagonal mesh that keeps large-area gratings supported (see Fig. 3).

2.3 Diffraction efficiency

We use rigorous coupled-wave analysis (RCWA) to model and predict diffraction efficiency (DE) for CAT grating structures. Our RCWA implementation assumes an infinite periodic grating that can be described as a sequence

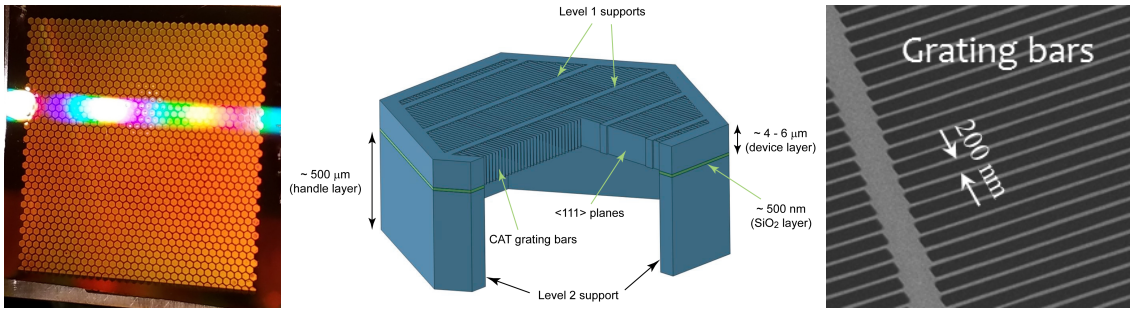

Figure 3. Left: Photograph of an existing 32 x 32 mm^2 CAT grating membrane with back illumination to show the hexagonal L2 mesh, and with visible light diffraction due to the L1 device layer mesh. Middle: Schematic showing the structural hierarchy (not to scale). Right: Top down SEM of grating membrane, showing thin grating bars and high throughput ($\sim$ 90%) L1 supports;

of stratified layers with constant index of refraction, and distinct regions of different indices of refraction within each grating layer. The simplest model consists of semi-infinite vacuum substrate and superstrate layers, and a single grating layer in between of depth d and with a silicon (width b) and a vacuum (width $p - b$) region. The interfaces between regions and layers are sharp (i.e. interface roughness $\sigma = 0$). This is an idealized model of a real CAT grating, where b may vary locally along each grating bar (line edge roughness) and over larger distances across the grating (contrast variations in lithography, uneven etch rates, etc.). Grating depth d can vary due to device layer thickness variations, sidewall roughness is finite, and the grating bar cross-sectional profile is not a perfect rectangle. Nevertheless we have been able to predict DE well and found good agreement between measurements and theory over many measurement campaigns.[7,16–18] Generally, we find DEs in the range of 85-100% of theoretical predictions. Near the critical angle performance falls off faster than predicted, which can be described reasonably well with an empirical Debye-Waller-like factor due to interface roughness. The impact of L1 and L2 structures can generally be described as absorption or blockage in proportion to the fractional area occupied by these structures. The latest generation of Arcus-like gratings delivers $> 30\%$ absolute DE (sum of diffraction orders 3-8, including L1 and L2 absorption) near a wavelength of $\lambda = 2.4$ nm, and a useful bandpass of $\lambda \sim$ 1-5 nm, which enables Arcus to reach its effective area goals.

2.4 Optical design and resolving power

By placing diffraction gratings on the surface of a Rowland torus that contains the telescope focus and the spectral readout sensors one can achieve the narrowest spectral lines and the highest resolving power R. It is predominantly limited by the telescope PSF, the subaperture angle subtended by the grating array, precision placement and alignment of the gratings, grating size, and grating period variations. Since CAT gratings are tilted relative to the incident x rays we have adapted a tilted Rowland torus design described previously.[8,9,11,19]

Using a Wolter-I slumped glass x-ray mirror pair (subapertured line spread function (LSF) $\sim$ 1 arcsec (FWHM), $\sim$ 9 m focal length) and a $\sim 10 \times 30$ mm^2 Pt-coated CAT grating we experimentally demonstrated $R > 10,000$ in 18$^{\text{th}}$ order using the Al K$\alpha_1\alpha_2$ doublet.[20,21] This shows that the CAT gratings of today are compatible with optical designs that provide $R > 10,000$.

2.5 Alignment and integration

The size of the grating arrays for Arcus and Lynx by far exceed sample sizes for fabrication tools, and the curvature of the Rowland torus requires curved grating arrays. This is best achieved in good approximation by tiling the grating array with many small, flat co-aligned gratings. We recently developed UV laser-based grating alignment methods[22,23] and demonstrated grating roll alignment to within better than 5 arcmin for an array of four 32×32 mm^2 gratings, and $R > 3500$ with an optics LSF of $\sim$ 2.1 arcsec (FWHM).[7] In collaboration with Harvard Smithsonian Astrophysical Observatory we have integrated our alignment metrology into a grating facet assembly station that bonds the silicon membranes made from SOI wafers onto narrow, flexure-based Ti frames.[7] Membrane and frame comprise a grating facet that can be placed anywhere on the Arcus grating array.

2.6 Environmental testing

Two CAT gratings bonded to frames underwent thermal cycling under vacuum and one of them additional vibration testing in air. Resolving power and DE were measured before and after testing, and no loss in performance was detected.[24] This gives us confidence that CAT gratings can survive launch and the space environment, but of course more testing will be performed in the future as design changes are introduced.

2.7 Ray tracing

Ray tracing is a traditional and essential tool for x-ray telescope design. Over the years we have produced ray trace models of increasing fidelity that allow us to predict spectrometer performance with high confidence and to develop realistic error budgets for resolving power and effective area.[8,9,11,19,25]

3. FROM ARCUS TO LYNX

Lynx is an ambitious x-ray mission concept for the 2030's. Despite its large mirror collecting area, today's CAT gratings cannot provide the required effective area, even if the grating array covers the whole mirror aperture.[11] The design for the Lynx CAT grating spectrometer assumes realistic future improvements in grating throughput and increases in grating size that will only require $\sim 2/3$ mirror coverage with a reasonable number of grating facets. Table 1 compares parameters for the Arcus and Lynx missions. If any of the listed Lynx parameters cannot be achieved there is 50% margin on the mirror aperture coverage that can be utilized without compromising the resolving power requirement.

Mission	R	A_{eff}	d	θ*	d.c.	L1	L2	L3	total	DE	size
		[cm^2]	[μm]	[deg]	b/p	trans.	trans.	trans.	trans.		[mm^2]
Arcus	> 2500	> 250	4.0	1.9	0.3	0.82	0.81	0.7	0.46	> 0.35	28×29
Lynx	> 5000	> 4000	5.75	1.6	0.2	> 0.9	> 0.9	0.98**	> 0.79	> 0.50	60×60

Table 1. Comparison between Arcus and Lynx for grating spectrometer requirements and CAT parameters for 200 nm period gratings. *Optimum blaze angle for given grating bar depth and duty cycle (d.c.). **L3 structures assumed to be mostly shadowed by mirror support structures.

Increasing transmission through the L1 and L2 structures simply means reducing their fractional area perpendicular to the direction of x-ray propagation. An example can be seen in the right side of Fig. 3, where we already fabricated a freestanding CAT grating with $< 10\%$ blockage from the L1 mesh. We are investigating how far reduction and design of L1 and L2 structures can be pushed before launch survivability becomes a problem.

3.1 Increasing etch depth to 6 micrometers

The key to higher grating DE is to build an efficient structure for smaller incidence angles θ. Smaller θ requires deeper gratings. Our goal structure for Lynx has $d = 5.75$ μm deep gratings ($p = 200$ nm), for which RCWA predicts DE $> 50\%$. The higher the aspect ratio of the etched trench and the finer the pitch, the harder it is to obtain good quality etch results, and the narrower the process window becomes. We have been marginally successful in extending etch depth from 4 to 6 μm on our old DRIE tool and started to investigate more modern tools. Figure 4 shows a cross section through a recent deep etch of a bulk (100) Si wafer on a SOTA tool, extending beyond 6 μm in depth. The oxide mask was patterned at MIT Lincoln Labs. The etch shows excellent uniformity and grating bar profiles. On a (110) SOI wafer this etch would be followed by a short wet etch in KOH solution, which narrows the grating bars and straightens the sidewalls.

3.2 Controlling etch profile tilt variations

Blazed gratings enhance diffraction orders in the direction of specular reflection from the blazing surfaces. To control blazing therefore means to control the angle of the reflecting surfaces. For CAT gratings this is done by tilting the gratings relative to the incident x-ray beam, assuming that all the grating bar sidewalls are parallel to each other to within a certain tolerance, typically on the order of $\sim \pm 0.2$ degrees.

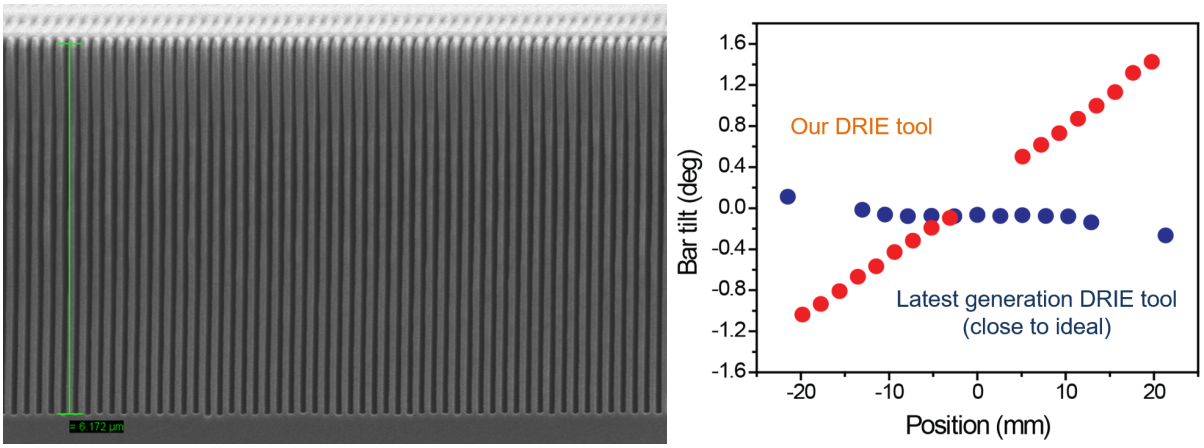

Figure 4. Left: Scanning electron micrograph of a cleaved 200 nm-period grating etched over 6 μm deep into bulk silicon on a SOTA DRIE tool. On the top the integrated orthogonal L1 cross supports are visible. Right: Etch profile tilt variations across a $>$ 40 mm-wide grating chip. Red: Results from our current, older generation DRIE tool. Blue: Results from the same tool that produced the etch in the left image. The outermost data points are affected by the proximity to the chip edges.

One potential source of sidewall angle variations is the deep etch step itself. Over small grating areas this is generally not a concern. However, for gratings on the order of several cm in size one cannot safely assume that the DRIE process is uniform enough to generate sufficiently parallel profiles all the way from one end of the grating to the other. We recently developed a fast, accurate and precise method based on small angle x-ray scattering to measure these etch profile tilt variations.[26] As seen on the right of Fig. 4, our old DRIE tool generates unacceptable, systematic variations in etch profile tilt across a few cm on a bonded wafer chip. In comparison, the same tool that was used for the etch in Fig. 4 provides almost negligible etch profile tilt variations.

3.3 Fabrication process development for large numbers of CAT gratings

Arcus requires $\sim$ 700 CAT gratings. Lynx requires $\sim$ 800-2000 CAT gratings, depending on the grating size we will be able to make with high yield. Currently we fabricate most CAT gratings from 100 mm SOI wafers one-by-one manually in a sequence of steps on tools available to us in a university setting. In order to make such a large number of high-precision components in a 1-2-year time frame available to these types of missions we can either scale this process up with many parallel stations, or we develop a process sequence that can take advantage of state-of-the-art fabrication tools from the semiconductor and MEMS industries. A dilemma is how to get access to such expensive tools for an extended length of time with a limited research budget in order to be able to do proper process development on such a different tool set. In nanofabrication trying to simply repeat a process developed on one tool on another tool - even if the tools are nominally identical - rarely works without troubleshooting and adjustments. Transferring a process onto a different, non-identical tool set can require a similar effort as the initial process development. For a mission to be successful these issues all have to be worked out well ahead of purchasing decisions and tool installation before high-yield mass production can begin.

We have recently begun a collaboration with the Microelectronics Group at MIT Lincoln Labs (LL). This group has automated coating, patterning and etching tools for the batch processing of 200 mm wafers. The initial pattern is generated in photoresist using 4X projection lithography using electron-beam written masks. Our goal is to transfer the fabrication of the oxide masks for DRIE to LL (see red box in Fig. 2), and to perform DRIE and subsequent processing in MIT campus labs. For Arcus the potential gains would be the fast batch production of oxide masks for 16-20 gratings/wafer with reliably repeatable results (e.g., repeatable DRIE mask duty cycle, line edge roughness, etc.), minimizing the need for process adjustments in the subsequent crucial and most sensitive front side DRIE step. Different tools and labs come with different limitations and requirements, and process transfer is not straightforward. Nevertheless, we recently have been able to successfully DRIE our first CAT gratings patterned at LL. Obtaining many gratings per wafer with good repeatability will allow us to

perform the systematic studies on different aspects of grating performance that are necessary to advance CAT grating TRL. For Lynx we require larger gratings, which are easier to fabricate from larger wafers. As gratings exceed $\sim$ 50 mm in size, aberrations begin to impact spectrometer resolving power. This can be mitigated by a small variation in grating period (grating "chirp"), which is straightforward to implement in projection lithography.[11] Currently the work with LL has come to a crawl due to limited funds.

4. OTHER CAT GRATING APPLICATIONS

CAT gratings are also considered as dispersing elements for a broadband soft x-ray polarimetry instrument.[27] This effort is led by the Marshall group at MIT, which has a 11-17 m long polarimetry beamline with a variety of electron bombardment targets for the characterization of optical elements in the x-ray band. CAT gratings have been tested there extensively. For some optical designs bending of CAT gratings (radius of curvature $\sim$1-2 m) is advantageous and has been demonstrated.[28]

5. DISCUSSION AND OUTLOOK

CAT grating technology has made great strides over the last decade. It is close to TRL 6 for Arcus purposes, and in many regards close to TRL 5 for Lynx. CAT grating DE is close to theoretical model predictions, $> 30\%$ near the astrophysically important O VII and O VIII lines, and predicted to be $> 50\%$ if grating depth is increased from 4 to 6 μm. Resolving power $R > 10,000$ has been demonstrated experimentally using 1.49 keV x rays. CAT gratings have been aligned into a four-facet array, spanning > 150 mm across, and demonstrated R in agreement with ray trace models. Environmental testing has not revealed any areas of concern.

We have now demonstrated the ability to etch CAT grating structures into Si beyond the depth required for Lynx on a SOTA demo DRIE etcher of a tool manufacturer. We need to repeat this work on (110) SOI wafers in order to make working CAT gratings. However, this is a highly impractical and inefficient endeavor to pursue on a remote demo tool. Similarly, demonstrating the predicted effective area in a breadboard or brassboard-type x-ray spectrometer setup requires gratings with bars that have parallel sidewalls across the whole extent of the grating. Fabricating such gratings also requires a SOTA DRIE tool. We are still investigating our options with regards to obtaining frequent and affordable access to such a tool.

Furthermore, to demonstrate progressively higher technology readiness levels, progressively larger grating arrays populated with progressively more flight-like gratings need to be fabricated, aligned, and integrated. This is a significant future effort that will require the fabrication of a significant fraction of the total required number of gratings. In order to demonstrate that the cost and schedule to produce the populated flight grating array are fully understood, the TRL 6 gratings need to be fabricated using essentially the same process and tool set as proposed for the flight gratings themselves. Analogous to the investments being made on tooling for the mass fabrication of the Lynx DRM silicon mirror segments,[29] for example, we need to start developing grating fabrication schemes now that are compatible with mass production.

ACKNOWLEDGMENTS

We gratefully acknowledge facility support from Microsystems Technology Labs and the Nanostructures Lab (both at MIT), the Microelectronics group at MIT Lincoln Labs, and Samco, Inc. This work made use of the Shared Experimental Facilities at MIT supported in part by the MRSEC Program of the National Science Foundation under award number DMR 1419807. This work was supported by NASA grant NNX17AG43G.

This paper is dedicated to Prof. Peter S. Pershan (Harvard University), a pioneer in the field of x-ray scattering studies of liquid surfaces and interfaces and thin liquid and organic films, on his 85$^{\text{th}}$ birthday.

REFERENCES

[1] Smith, R. K., *et al.* "Arcus: The soft x-ray grating Explorer," Proc. SPIE 11118 (these proceedings).
[2] Bautz, M. W., "The Lynx x-ray observatory: Science drivers," Proc. SPIE 11118 (these proceedings).
[3] C. R. Canizares *et al.*, "The Chandra high-energy transmission grating: Design, fabrication, ground calibration, and 5 years in flight," PASP **117**, 1144-1171 (2005).

[4] J. W. den Herder *et al.*, "The reflection grating spectrometer on board XMM-Newton," Astr. & Astroph. **365**, L7-L17 (2001).
[5] Collon, M. J., *et al.*, "Silicon pore optics mirror module production and testing," *Proc. SPIE* **11180**, 1118026 (2019).
[6] http://sci.esa.int/athena/
[7] Heilmann, R. K., *et al.*, "Blazed transmission grating technology development for the Arcus x-ray spectrometer Explorer ," *Proc. SPIE* **10699**, 106996D (2018).
[8] Günther, H. M., Heilmann, R. K., Cheimets, P., and Smith, R. K., "Performance of a double tilted-Rowland-spectrometer on Arcus," *Proc. SPIE* **10397**, 103970P (2017).
[9] Günther, H. M. *et al.*, "Ray-tracing Arcus in Phase A," *Proc. SPIE* **10699**, 106996F (2018).
[10] Gaskin, J. A., *et al.*, "Lynx x-ray observatory: An overview," *J. Astron. Telesc. Instrum. Syst.* **5**, 021001 (2019).
[11] Günther, H. M., and Heilmann, R. K., "Lynx soft x-ray critical-angle transmission grating spectrometer," *J. Astron. Telesc. Instrum. Syst.* **5**, 021003 (2019).
[12] https://www.lynxobservatory.com/
[13] https://wwwastro.msfc.nasa.gov/lynx/docs/documents/TechnologyRoadmaps/CAT_TR.pdf
[14] Bruccoleri, A. R., Guan, D., Mukherjee, P., Heilmann, R. K., Schattenburg, M. L. and Vargo, S., "Potassium hydroxide polishing of nanoscale deep reactive-ion etched ultra-high aspect ratio gratings," *J. Vac. Sci. Technol. B* **31**, 06FF02 (2013).
[15] Bruccoleri, A. R., Heilmann, R. K., and Schattenburg, M. L., "Fabrication process for 200 nm-pitch polished freestanding ultra-high aspect ratio gratings," *J. Vac. Sci. Technol. B* **34**, 06KD02 (2016).
[16] Heilmann, R. K., Ahn, M., Gullikson, E. M. and Schattenburg, M. L., "Blazed high-efficiency x-ray diffraction via transmission through arrays of nanometer-scale mirrors," *Opt. Express* **16**, 8658-8669 (2008).
[17] Heilmann, R. K., Ahn, M. and Schattenburg, M. L., "Fabrication and performance of blazed transmission gratings for x-ray astronomy," *Proc. SPIE* **7011**, 701106 (2008).
[18] Heilmann, R. K., Ahn, M., Bruccoleri, A., Chang, C.-H., Gullikson, E. M., Mukherjee, P. and Schattenburg, M. L., "Diffraction efficiency of 200 nm period critical-angle transmission gratings in the soft x-ray and extreme ultraviolet wavelength bands," *Appl. Opt.* **50**, 1364-1373 (2011).
[19] Heilmann, R. K. *et al.*, "Critical-angle transmission grating spectrometer for high-resolution soft x-ray spectroscopy on the International X-Ray Observatory," *Proc. SPIE* **7732**, 77321J (2010).
[20] Heilmann, R. K., Bruccoleri, A. R., Kolodziejczak, J., Gaskin, J. A., ODell, S. L., Bhatia, R., and Schattenburg, M. L., "Critical-angle x-ray transmission grating spectrometer with extended bandpass and resolving power $> 10,000$," *Proc. SPIE* **9905**, 99051X (2016).
[21] Heilmann, R. K., Kolodziejczak, J., Bruccoleri, A. R., Gaskin, J. A., and Schattenburg, M. L., "Demonstration of resolving power $\lambda/\Delta\lambda > 10,000$ for a space-based x-ray transmission grating spectrometer," *Appl. Opt.* **58**, 1223-1238 (2019).
[22] Song, J., Heilmann, R. K., Bruccoleri, A. R., Hertz, E., and Schattenburg, M. L., "Scanning laser reflection tool for alignment and period measurement of critical-angle transmission gratings," *Proc. SPIE* **10399**, 1039915 (2017).
[23] Song, J., Heilmann, R. K., Bruccoleri, A. R., Hertz, E., and Schattenburg, M. L., "Metrology for quality control and alignment of CAT grating spectrometers," *Proc. SPIE* **10699**, 106990S (2018).
[24] Heilmann, R. K., *et al.*, "Critical-angle transmission grating technology development for high resolving power soft x-ray spectrometers on Arcus and Lynx," *Proc. SPIE* **10399**, 1039914 (2017).
[25] Davis, J. E., *et al.*, "Raytracing with MARX X-ray observatory design, calibration, and support," *Proc. SPIE* **8443**, 84431A (2012).
[26] Song, J., Heilmann, R. K. and Schattenburg, M. L., "Characterizing profile tilt of nanoscale deep-etched gratings via x-ray diffraction," submitted to *J. Vac. Sci. Technol. B.*
[27] Marshall, H. L., *et al.*, "Design of a broadband soft x-ray polarimeter," *J. Astron. Telesc. Instrum. Syst.* **4**, 011005 (2018).
[28] Garner, A., *et al.* "Component testing for x-ray spectroscopy and polarimetry," Proc. SPIE 11118 (these proceedings).
[29] Zhang, W. W., *et al.*, "High-resolution, lightweight, and low-cost x-ray optics for the Lynx observatory," *J. Astron. Telesc. Instrum. Syst.* **5**, 021012 (2019).